

pubs.acs.org/JACS Article

On the Mechanism of the Inverse Vulcanization of Elemental Sulfur: Structural Characterization of Poly(sulfur-random-(1,3-diisopropenylbenzene))

Jianhua Bao, Kaitlyn P. Martin, Eunkyung Cho, Kyung-Seok Kang, Richard S. Glass, Veaceslav Coropceanu, Jean-Luc Bredas, Wallace O'Neil Parker, Jr.,* Jon T. Njardarson,* and Jeffrey Pyun*



Cite This: J. Am. Chem. Soc. 2023, 145, 12386-12397



ACCESS

III Metrics & More

Article Recommendations

s Supporting Information

ABSTRACT: Organosulfur polymers, such as those derived from elemental sulfur, are an important new class of macromolecules that have recently emerged via the inverse vulcanization process. Since the launching of this new field in 2013, the development of new monomers and organopolysulfide materials based on the inverse vulcanization process is now an active area in polymer chemistry. While numerous advances have been made over the last decade concerning this



polymerization process, insights into the mechanism of inverse vulcanization and structural characterization of the high-sulfur-content copolymers that are produced remain challenging due to the increasing insolubility of the materials with a higher sulfur content. Furthermore, the high temperatures used in this process can result in side reactions and complex microstructures of the copolymer backbone, complicating detailed characterization. The most widely studied case of inverse vulcanization to date remains the reaction between S₈ and 1,3-diisopropenylbenzene (DIB) to form poly(sulfur-random-1,3-diisopropenylbenzene)(poly(S-r-DIB)). Here, to determine the correct microstructure of poly(S-r-DIB), we performed comprehensive structural characterizations of poly(S-r-DIB) using nuclear magnetic resonance spectroscopy (solid state and solution) and analysis of sulfurated DIB units using designer S-S cleavage polymer degradation approaches, along with complementary *de novo* synthesis of the sulfurated DIB fragments. These studies reveal that the previously proposed repeating units for poly(S-r-DIB) were incorrect and that the polymerization mechanism of this process is significantly more complex than initially proposed. Density functional theory calculations were also conducted to provide mechanistic insights into the formation of the derived nonintuitive microstructure of poly(S-r-DIB).

■ INTRODUCTION

The use of elemental sulfur (S_8) as alternative, commodity feedstock for polymer synthesis has become an attractive technological aim to sustainably create high-value chemical products. 1-3 While this endeavor is incentivized by the largescale generation of S₈ from petroleum refining, the dearth of synthetic polymerization methods to directly employ elemental sulfur as a monomer has hindered significant advances in this area. Furthermore, discernable structure-property advances of S₈-derived polymers vs those of classical commodity hydrocarbon-based polymers have historically been lacking, which stifled research of high-sulfur content polymeric materials. A notable early exception in this field was the elegant work of Penczek et al. on anionic ring-opening copolymerization of S₈ with propylene sulfide.^{4,5} While the melt, homolytic ringopening polymerization (ROP) of S₈ has long been known to undergo equilibrium polymerization, 6,7 the concept of using liquid sulfur as a comonomer reaction medium had not been developed.

A major advance in this area was the development of a new polymerization process termed inverse vulcanization, which enabled the bulk copolymerization of molten elemental sulfur and unsaturated comonomers without the need for externally added initiators or solvents. The inverse vulcanization process proceeds at elevated temperatures where the equilibrium between S_8 (also other cyclic forms) and ring-opened sulfur diradicals drives the polymerization (Figure 1). A diverse range of unsaturated organic comonomers have been investigated for inverse vulcanization in the past decade, which include styrenes, α -methyl styrenes, cyclic olefins, natural olefinic products, allyls, alkynes, and benzoxazines, 2,7,9,10 as well as aliphatic benzylic comonomers. A common major

Received: April 6, 2023 Published: May 24, 2023





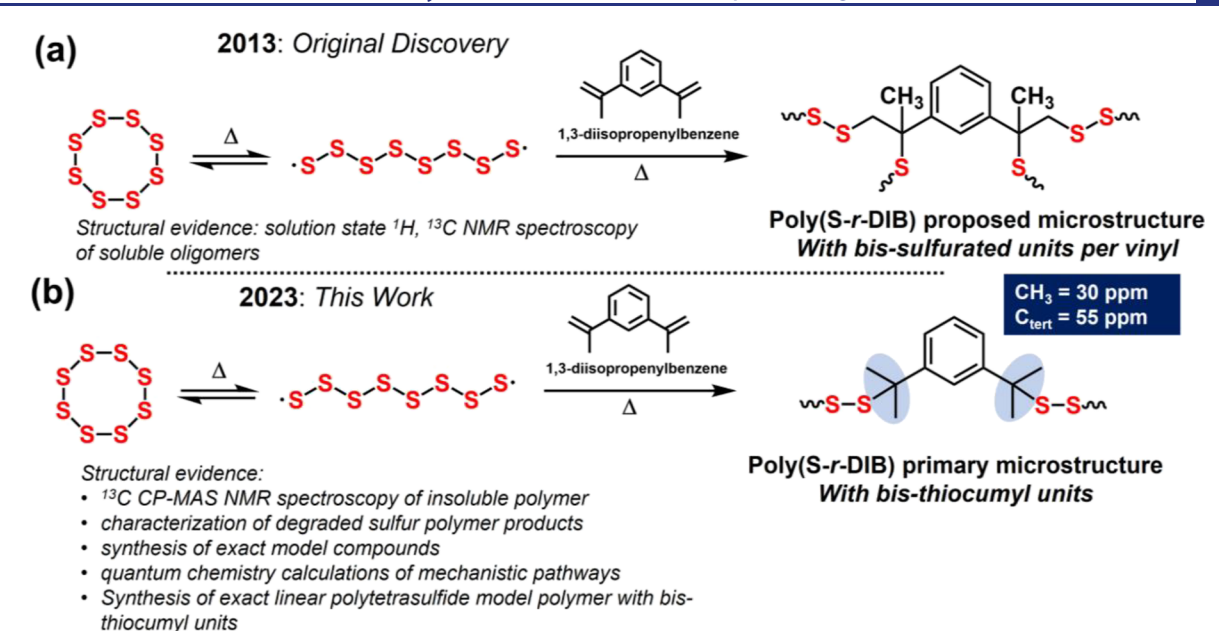


Figure 1. Proposed microstructures for poly(S-r-DIB) from the inverse vulcanization of S_8 with DIB: (a) previously proposed microstructure from the original discovery of Pyun et al. and (b) revised bis-thiocumyl microstructure.

obstacle in screening new organic comonomers is poor miscibility with liquid sulfur, which greatly narrows the scope of accessible comonomers for inverse vulcanization. Recently reported efforts to expand the scope include the use of liquid sulfur resins as prepolymers for dynamic covalent polymerization (DCP), 12–16 organic nucleophilic activators, 14,17,18 organo/metal salt dithiocarbamate catalysts, 19,20 or photo-induced processes. 21,22

High sulfur content organosulfur copolymers made via inverse vulcanization have been referred to by different names such as inverse vulcanized polymers and chalcogenide hybrid inorganic/organic polymers (CHIPs), both of which refer to sulfur copolymers with a statistical sequence of S-S bonds in a copolymer backbone with organic comonomers.9 The high sulfur content of these polymers has imparted intriguing optical and electrochemical properties for emerging applications in infrared optics, ^{23–32} Li–S batteries, ^{8,33–40} self-healing materials, ^{24,41–43} environmental remediation, ^{44–47} agrochemical fertilizers, ⁴⁸ adhesives, ⁴⁹ thermoplastic elastomers, ¹⁵ rubber vulcanization agents, ^{16,50} and flame retardant materials, ¹⁵ and flame retardant materials. als. 15,51 While the inclusion of S-S bonds imparts unusual properties to these materials, it also renders these polymers intractable, which has complicated structural characterization of these materials. To date, either solid-state ¹³C NMR spectroscopy of sulfur polymers or solution-state NMR spectroscopy characterization of soluble, oligomeric forms of these materials has been conducted to identify the copolymer microstructures.

It has been a decade since the pioneering development of the inverse vulcanization of S_8 with 1,3-diisopropenylbenzene (DIB), which has since been highly followed. Poly(sulfur-random-1,3-diisopropenylbenzene) (poly(S-r-DIB)) has become one of the most widely studied high-sulfur-content polymeric materials derived from the inverse vulcanization of S_8 . The repeating unit proposed from poly(S-r-DIB) was initially reported by Pyun et al. using soluble oligomers by solution 13 C NMR spectroscopy; it was posited that the reaction proceeds via a thiyl radical addition to vinyl groups of DIB followed by coupling of the resulting radical with thiyl

radicals, or ring opening of S₈, affording a polymer microstructure repeating unit consisting of -S-CH₂-C(CH₃)(Ph-R)—S bis-sulfurated groups (Figure 1a). Subsequent solid-state ¹³C NMR spectroscopic characterization by cross-polarization magic angle spinning (CP-MAS) NMR spectroscopy of poly(S-r-DIB) was conducted which also seemed to support this proposed microstructure. 52,53 The limited solubility of poly(S-r-DIB) has complicated more detailed NMR spectroscopic studies of the exact microstructure of this new material, along with spinning side band issues that easily arise for ¹³C CP-MAS NMR spectroscopy; this further confounded an unambiguous structural assignment of the correct repeating unit structure of this high sulfur content polymer. Furthermore, the synthesis and isolation of bis-thiol or tertiary thiols that can serve to model compounds for NMR spectroscopic analysis are nontrivial to conduct due to oxidative stability issues to form disulfide products, which has further hampered work on this important question.

Herein, we report a complete study on the structural characterization of poly(S-r-DIB) derived from inverse vulcanization through a combination of solid-state NMR spectroscopy of the insoluble polymer and solution-state NMR spectroscopic studies of degraded organic units from the same polymer. Essential to these studies is suppression of spinning side bands in the ¹³C CP-MAS NMR spectroscopic measurement, along with cross-polarization spectral editing (CP-editing) and T₁ relaxation experiments of bona-fide ¹³C resonances from the material. We further report on synthesis of exact model bis-thiol compounds to match the new proposed repeating unit structure for poly(S-r-DIB). These studies reveal that the primary microstructure of poly(S-r-DIB) is a bisthiocumyl fragment (Figure 1b), which represents a profound departure from the initially proposed microstructures. Importantly, we demonstrate that we can engage this bisthiol model compound with sulfur monochloride (S₂Cl₂) to prepare precise linear polytetrasulfide model polymers, for comparison with the structure and properties of inverse vulcanization-derived poly(S-r-DIB), to corroborate the

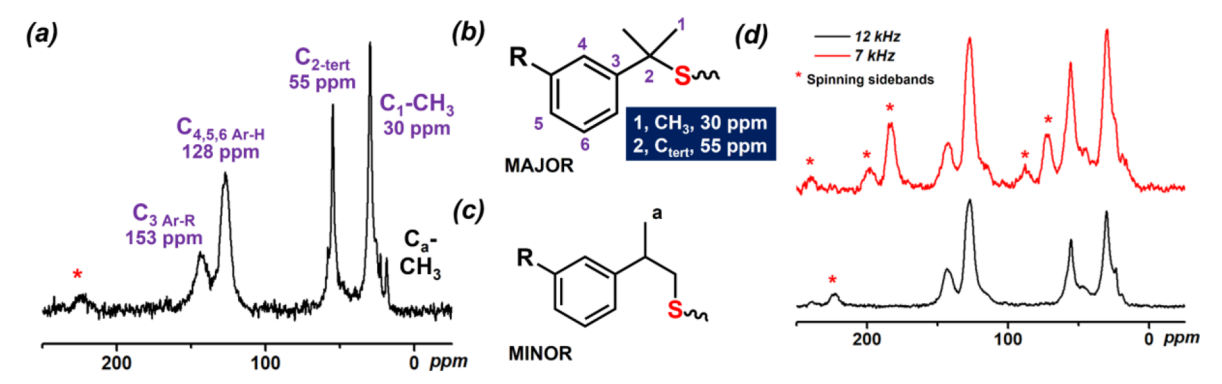


Figure 2. (a) Solid-state ¹³C cross-polarized magic angle spinning (CP-MAS) nuclear magnetic resonance (NMR) spectrum (12 kHz) of insoluble poly(S-r-DIB) with signal assignments. Large 128 ppm signal, from aromatic CH carbons, gives small spinning side-bands at 222 ppm (red asterisks), (b) chemical structure of the MAJOR thiocumyl fragment labeled with peaks from Figure 2a, (c) chemical structure of the MINOR thiopropyl fragment from (a), and (d) solid-state ¹³C CP-MAS NMR spectrum of insoluble poly(S-r-DIB) measured at different spinning rates (7, 12 kHz) to show these effects on spinning side band peaks.

corrected structure. Access to these key bis-cumyl tertiary thiols allows facile designer synthesis of polytetrasulfides of exact sulfur rank via a powerful union with sulfur monochloride (S₂Cl₂). Finally, density functional theory (DFT) calculations provide mechanistic insights into the polymerization pathways that afford poly(S-r-DIB) from inverse vulcanization.

■ RESULTS & DISCUSSION

Solid-State NMR Spectroscopy of Poly(S-r-DIB). ¹³C CP-MAS NMR spectroscopic characterization of poly(S-r-DIB) was initially conducted to investigate the predominant carbon atoms and functional fragments observed in the polymer. For the current study, poly(S-r-DIB) with a 50-wt % sulfur composition was prepared by inverse vulcanization at either 160 or 185 °C followed by isolation of the wholly insoluble fraction of this material (~60-wt % of crude product) to afford purified materials for solid-state NMR spectroscopy. Computationally predicted ¹³C chemical shifts of the fully sulfurated "idealized" bis-sulfurated microstructure for poly(Sr-DIB) of the aliphatic carbons of the sulfur copolymer backbone afford predicted resonances at 29 ppm for methyl carbons, 51 ppm for methylene carbons, and 60 ppm for the tertiary carbons. What is immediately apparent in the ¹³C CP-MAS NMR spectrum of poly(S-r-DIB) is the contrast with this idealized microstructure as noted by the observation of two major ¹³C resonances corresponding to a methyl signal (30 ppm) possessing a peak area nearly twice that of the Ctert tertiary carbon (55 ppm) and the absence (or trace amounts) of methylene carbon resonances which points to the formation of a mono-sulfurated branched thiocumyl fragment in the copolymer microstructure (Figure 2a,b). Addition of thiyl radicals to the isopropenyl olefin followed by sulfur trapping of resulting radical intermediate with thiyl, or S-S species would afford two C-S bonds and give rise to the -S-CH₂methylene and -S-C(CH₃)(Ph)- fragments as depicted for the idealized bis-sulfurated microstructure (Figure 1a). A significantly less abundant methyl carbon signal (20 ppm) is also observed, which points to the formation of another minor poly(S-r-DIB) microstructure suggestive of a mono-sulfurated linear propyl fragment (Figure 2a,c). ¹³C resonances at 128 and 153 ppm are due to the aromatic carbons of the DIB ring which match as expected the corresponding solution-state ¹³C NMR spectroscopic assignments for the DIB monomer. A

critical experimental parameter in this analysis is the effect of the spinning rate during ¹³C CP-MAS NMR spectroscopic analysis of poly(S-r-DIB), which we delineate by variation of frequency from 7-12 kHz. While the ¹³C CP-MAS NMR spectroscopy of poly(S-r-DIB) has been investigated,⁵³ nonoptimal sampling conditions continue to confound accurate structural assignment of insoluble S₈-derived polymeric materials. As illustrated in Figure 2d (red line higher spectra), the ¹³C CP-MAS NMR spectrum of poly(S-r-DIB) collected at 7 kHz exhibits numerous spinning side bands (from the two aromatic signals) at 230, 195, 185, 90, and 87 ppm, which are largely eliminated by spinning at 12 kHz (Figure 2d, black line lower spectra). Elimination of these large spinning side bands seems obvious but is a nontrivial condition to accurately discern the correct microstructures for poly(S-r-DIB). Finally, longitudinal (T₁) relaxation (see Supporting Information, Figures S25-27) and spectral editing (Figure S30) ¹³C CP-MAS NMR measurements of poly(S-r-DIB) carbons were made for each ¹³C resonance shown in Figure 2a to confirm assignment of methyl and tertiary carbons and the absence of methylene carbons not reported previously. The collective findings of these solid-state NMR spectroscopic investigations indicate that the primary microstructure of poly(S-r-DIB) is constituted of bis-thiocumyl units, with a minimal contribution of a minor microstructure of mono-thiolated propyl units, which unambiguously points to an alternative polymerization mechanism for the inverse vulcanization process than previously proposed.

Solution-State NMR Spectroscopy of Model Compounds and Degraded Polymer Products. To further corroborate the surprising structural findings from solid-state NMR spectroscopy, designer reductive S-S bond degradation of poly(S-r-DIB) and solution-state NMR spectroscopic characterization of the resulting isolated thiolated DIB products were conducted to provide unambiguous reference solution NMR spectra. Furthermore, synthesis of exact model compounds was performed to provide accurate reference spectra for NMR analytical assignments and comparisons with degraded products. After surveying reagents and conditions most suitable to efficiently cleave all sulfur-sulfur (S-S) bonds for insoluble poly(S-r-DIB) materials, 54,55 lithium aluminum hydride (LiAlH₄) emerged as best suited for this chemo-selective reductive degradation. Toward that end, the insoluble sulfur copolymer was suspended in dry tetrahy-

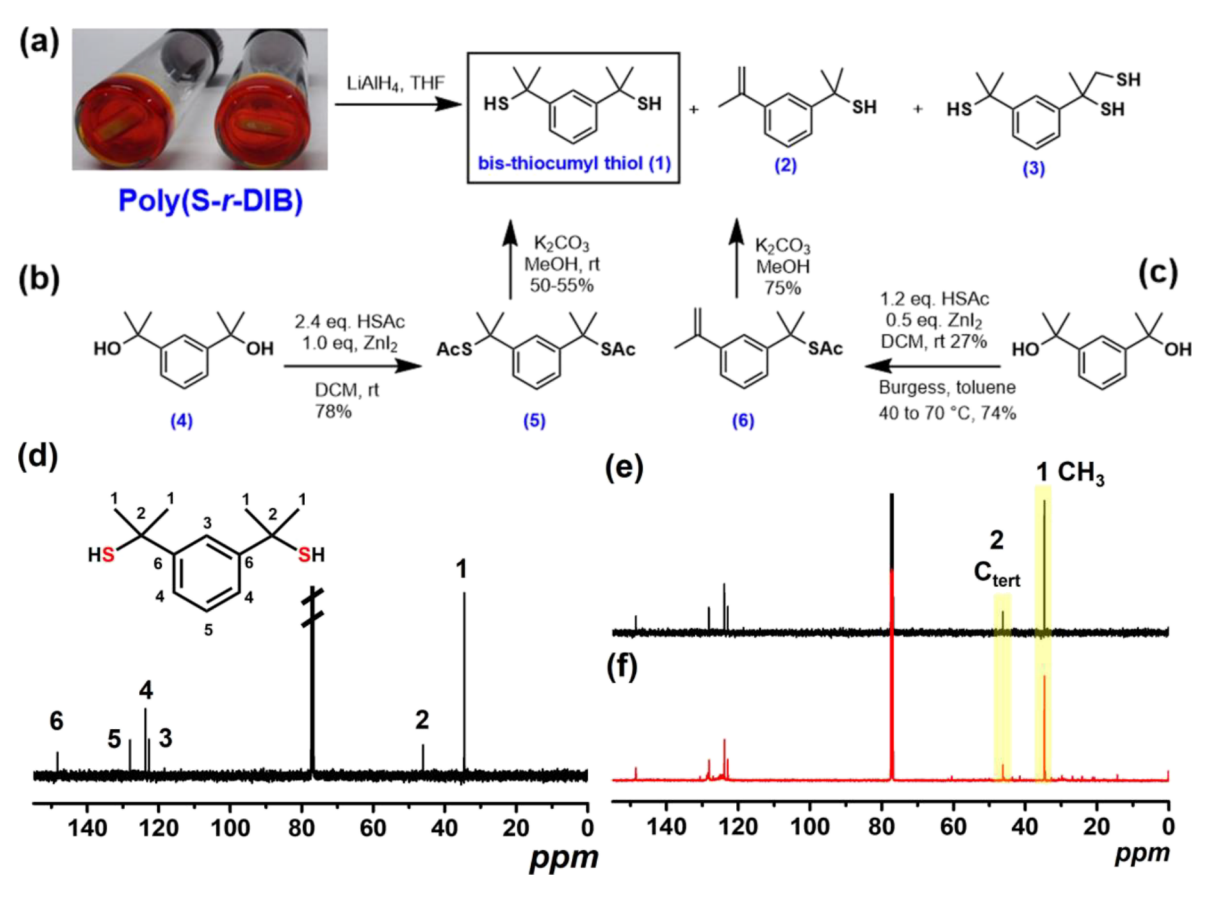


Figure 3. (a) Synthesis scheme for the reductive degradation of the insoluble poly(S-r-DIB) with LiAlH₄, (b, c) synthetic schemes for model compounds bis-cumyl thiol 1 and cumyl thiol 2, (d) solution-state 13 C NMR spectra of bis-cumyl thiol 1 with labeled structure of carbons C_1 – C_6 , and (e) solution 13 C NMR spectra of bis-cumyl thiol 1 overlayed with (f) solution 13 C NMR spectra of the crude degradation products of the insoluble poly(S-r-DIB) after LiAlH₄ reduction with –CH₃ (35 ppm), and –C_{tert} (46 ppm) peaks highlighted in yellow.

drofuran (THF) and treated with LiAlH₄ overnight at room temperature wherein it became homogeneous. Isolation of the sulfurated DIB degraded units was achieved by acidic workup, multiple extractions, and separation by silica gel chromatography to afford thiols 1, 2, and 3 for characterization by solution state ¹H and ¹³C NMR spectroscopy (Figure 3a). This reductive degradation protocol revealed that the major product formed from this reaction was bis-cumyl thiol 1 (Figure 3a) as these were almost exclusively the peaks (CH₃, 35 ppm; C_{tert}, 46 ppm) observed from solution-state ¹³C NMR spectroscopy of the reduced poly(S-r-DIB) crude mixture before silica gel purification (Figure 3f). The solution-state ¹³C NMR spectra of these degraded DIB units also tracked closely to the bisthiocumyl fragment observed in the ¹³C CP-MAS NMR spectra from poly(S-r-DIB) (Figure 2a). Furthermore, two additional thiol compounds were recovered (2, 3), which were observed in the solution ¹H and ¹³C NMR spectra of the degraded mixture; these corresponded to minor microstructure fragments in the sulfur copolymers, as inferred from the isolated yields relative to the bis-cumyl thiol 1 (Figure 3a and Supporting Information). These minor products (2, 3) were identified as a degraded DIB unit bearing a single thiocumyl group in addition to either an isopropenyl or bis thiol group (Figure 3a). Thiol 2 could be most readily attributed to terminal units of the poly(S-r-DIB) copolymer with dangling vinyl groups. Conversely, thiol 3 containing both thiocumyl and bis-thiol units points to a very minor contribution of the "idealized" bis-sulfuration of an olefinic unit as shown in Figure

1a. Comparative analysis of the soluble phase of poly(S-*r*-DIB) recovered after washing of the crude product initially afforded more complex solution ¹³C NMR spectra than observed for the solid state ¹³C NMR spectra of the insoluble fraction (shown in Figure 2a); however, after reductive degradation of this soluble poly(S-*r*-DIB) mixture with LiAlH₄ in THF, similar solution ¹³C NMR spectra were obtained, which also revealed the predominant formation of bis-cumyl thiol 1 (see Supporting Information, Figure S41).

Independent syntheses of model compounds 1 and 2 were conducted to unambiguously confirm the structures of the organic fragments (Figure 3b,c). Tertiary thiols are historically challenging to prepare, with synthetic methods for bis-tertiary thiol representing a neglected area with few available choices. Furthermore, it is important to note that isolation of these dithiols for structural characterization is challenging due to rapid oxidative coupling reactions to form disulfide byproducts. Treatment of 2,2'-(1,3-phenylene)bis(propan-2-ol) 4 with thioacetic acid (HSAc) in the presence of zinc(II) iodide (ZnI₂)⁵⁶ in dichloromethane (DCM) converted the two tertiary benzylic alcohols into bis-thioacetates (5, 6), which were then cleaved with potassium carbonate (K2CO3) in methanol to form bis-cumyl thiol 1 (Figure 3b). The solutionstate ¹³C NMR spectrum of 1 (Figure 3d) gratifyingly matched the peaks in the ¹³C NMR spectrum of the insoluble poly(S-r-DIB) material after LiAlH₄ reduction as most notably observed in stacked ¹³C NMR spectra of the model compound 1 and the crude degradation mixture (Figure 3e,f). Furthermore, the

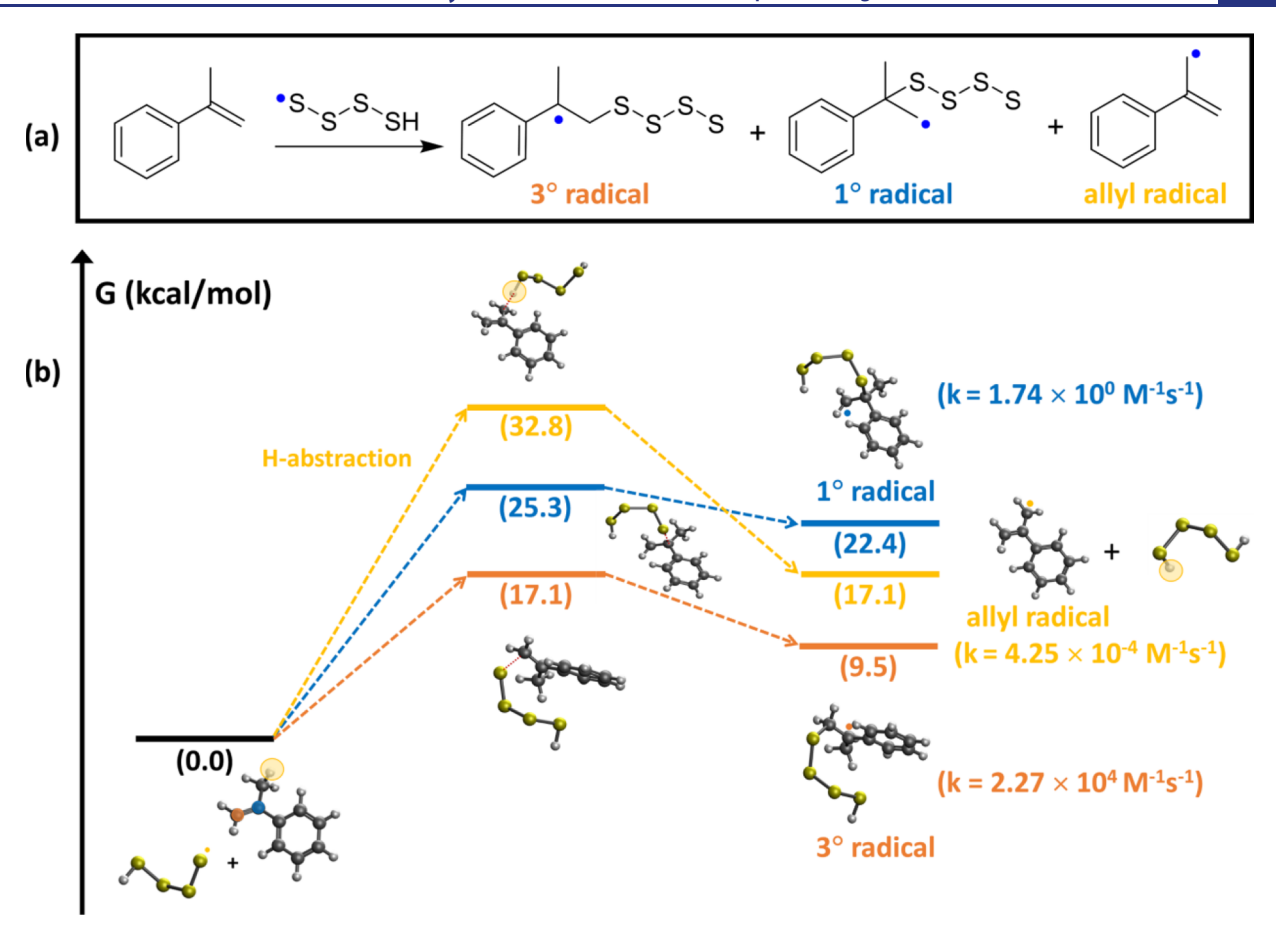


Figure 4. (a) Reaction schemes considered in the DFT/M06-2X calculations of tetrasulfane thiyl radical to MeSty via thiol-ene, or H-atom abstraction pathways and (b) reaction coordinate profile for the possible reactions of tetrasulfane thiyl radical to MeSty.

same bis-cumyl thiol 1 could also be converted to a monothioacetate wherein the unreacted tertiary alcohol converted into a propenyl group using the Burgess dehydration protocol (Figure 3c).⁵⁷ Hydrolysis of the thioacetate completed the independent synthesis of 2, whose analytical data matched those of the minor poly(S-*r*-DIB) organic fragment degradation product.

These collective findings corroborate the correct assignment of the primary microstructure of poly(S-r-DIB) to be the bisthiocumyl unit with one C-S bond per vinyl group. While the spectroscopic and experimental studies for poly(S-r-DIB) prove the formation of bis-thiocumyl units, numerous mechanistic questions remain on the formation of these thiocumyl units where only one C-S bond is formed per isopropenyl group in DIB. Furthermore, conversion of isopropenyl groups to thiocumyl fragments requires one additional H-atom per each olefinic moiety (2H-atoms per DIB molecule), where the only sources of H-atoms are the DIB monomers themselves since inverse vulcanization is conducted as a bulk, addition polymerization. The formation of thiocumyl fragments can be rationalized by the thiyl radical addition to the tertiary olefinic carbon of the DIB vinyl groups, affording a primary methylene radical that could in principle be terminated by -SSH sulfane species in the molten sulfur media. Chemically similar organohydropersulfides have been reported to be highly reactive H-atom donors toward both thiyl and alkyl radical species.⁵⁸ While this regiochemistry appears unfavorable, similar regiochemistry was observed for the inverse vulcanization of S₈ with styrene by solution ¹H

NMR spectroscopy of the soluble poly(S-r-Sty) material. Nevertheless, this is a dramatic mechanistic departure from the originally proposed mechanism for the inverse vulcanization of S_8 with DIB, which prompted quantum chemistry calculations to provide insights into this unusual polymerization processes.

Computational Modeling of the Inverse Vulcanization of S₈ and DIB. DFT calculations at the M06-2X/6-31 + G** level with the Gaussian 16 package⁶⁰ were conducted using α -methyl styrene (MeSty) and tetrasulfane⁶¹ thiyl radical species (H-S-S-S-S, Figure 4) as the reactants to model the inverse vulcanization of S₈ and DIB. These calculations afforded the Gibbs free energies (G) of possible intermediates and the transition states of the proposed reaction pathways of interest, along with the reaction rates of most likely reaction pathways (Figures 4-567). Frequency analyses followed by geometry optimizations were conducted at the same level of theory to confirm the nature of the stationary points; minima, such as those corresponding to reactants or products, have zero imaginary frequencies while transition states (TS) have one imaginary frequency corresponding to a saddle point on the reaction potential energy surface. For TS calculations, intrinsic reaction coordinate analyses were carried out. The rate constants for the reaction were calculated as $k(T) = \kappa \frac{k_{\rm B}T}{hc} e^{-\Delta G_{\rm a}^{\dagger}/RT}$ where $k_{\rm B}$, h, and R denote Boltzmann's constant, Planck's constant, and the ideal gas constant, respectively; T is the reaction temperature (taken here as 433 K, i.e., 160 °C); ΔG_a^{\ddagger} is the Gibbs free energy of activation, i.e., the difference between the free energy of the reactant state

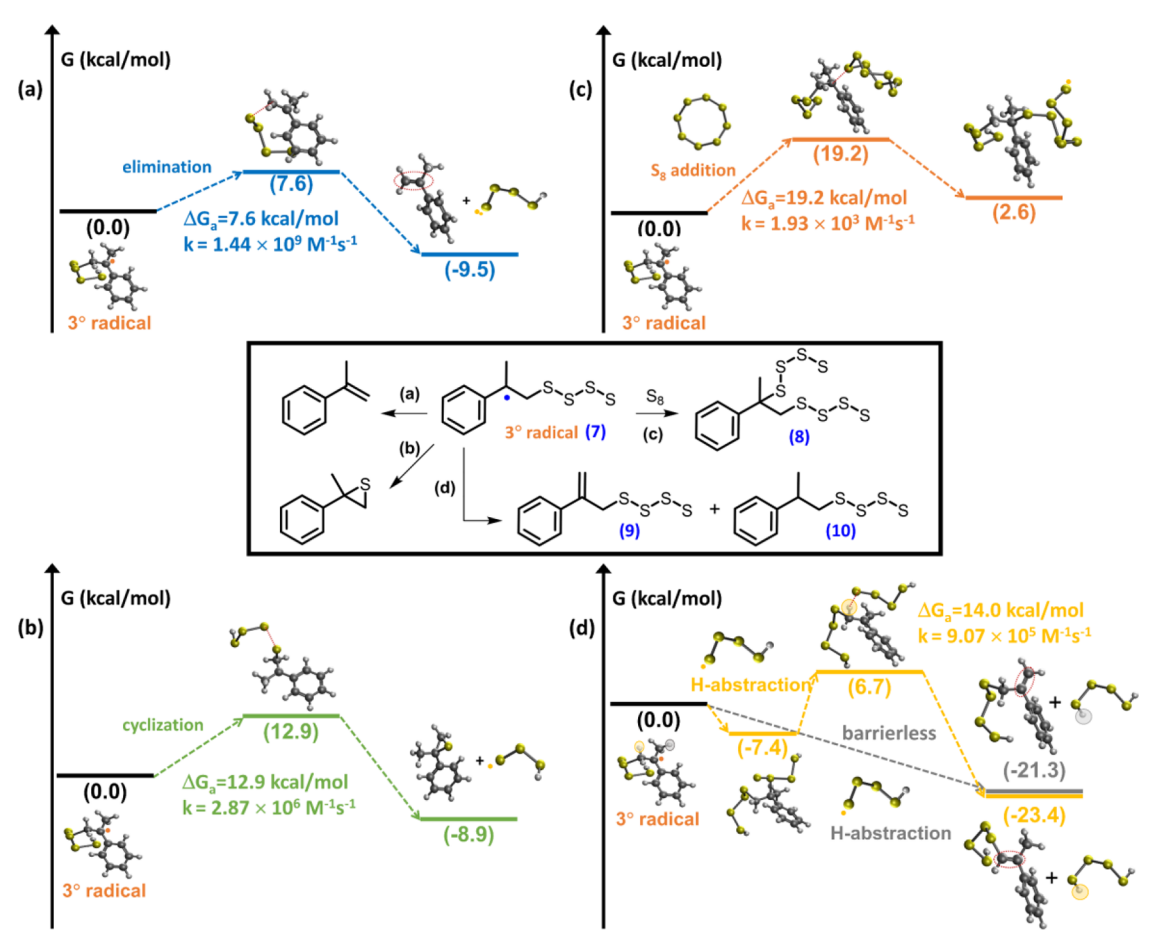


Figure 5. Center panel: Reaction scheme illustrating four possible reaction pathways for tertiary radical species 1 to undergo (a) elimination-depolymerization, (b) cyclization to thiirane, (c) ring-opening addition to S_8 , and (d) allylic H-atom abstraction from thiyl radical species to form allylic and vinyl sulfides.

and that of the TS; c denotes the concentration, which is conventionally set to be 1 M; $\kappa=1+\frac{1}{24}\Big(\frac{h\,\mathrm{Im}(\nu)}{k_{\mathrm{B}}T}\Big)^2$ is the tunneling correction factor based on the Wigner model and $\mathrm{Im}(\nu)$ is the imaginary frequency derived at the corresponding TS.

Simulations of Chemo- and Regioselectivity of Thiyl Radicals with α -Methyl Styrene. Computational studies were initially conducted for the reaction between MeSty and the tetrasulfane thiyl radical species (H-S-S-S-S), see Figure 4, to evaluate the energetics of thivl radical addition to form either a primary radical (color-coded in blue in the figure) or a tertiary radical (orange), along with an allylic radical (yellow), obtained from thiyl radical hydrogen abstraction from the allylic methyl group; we deemed these to be the most likely reaction scenarios between these two species (Figure 4a). Not surprisingly, formation of the tertiary radical, as observed in classical thiol-ene addition reactions (Figure 4a), is a significantly more favorable process than formation of the more sterically challenged cumyl-sulfide primary radical. Calculations support this chemical intuition as noted by lower energetic barriers for tertiary radical formation (ΔG_a^{\ddagger} =17.1 kcal/mol) vs generation of the primary radical (ΔG_a^{\ddagger} = 25.3 kcal/mol) and significantly faster reaction rates $(\sim 10,000 \times)$ for tertiary radical formation $(k = 2.27 \times 10^4)$ L/mol s vs $k = 1.74 \times 10^{0}$ L/mol s, Figure 4b). The competing thiyl radical hydrogen abstraction process to form protonated

H-S-S-S-H and MeSty allylic radicals was observed to be endergonic and to proceed with a significantly higher energetic barrier ($\Delta G_a^{\ddagger} = 32.8 \text{ kcal/mol}$) and slower reaction rates ($k = 4.25 \times 10^{-4} \text{ L/mol s}$) relative to both thiol-ene reaction pathways (Figure 4b). However, the calculated energies of the HSSSSH and MeSty allyl radical products $(\Delta G = 17.1 \text{ kcal/mol})$ were intermediate to those of the tertiary ($\Delta G = 9.5 \text{ kcal/mol}$) and primary ($\Delta G = 22.4 \text{ kcal/mol}$ mol) radical products, which will prove to be a significant finding, as will be detailed below (Figure 4b). Furthermore, the allylic hydrogen abstraction pathway affords a homolytic process to form -SSSSH sulfane species in situ which can serve as the H-donor species to form thiocumyl units, vide infra. The overall assessment of these initial bimolecular processes of thiyl radicals and MeSty indicates that the formation of the tertiary radical tetrasulfide adduct is the predicted addition product. However, since these types of microstructures are NOT observed experimentally for poly(Sr-DIB), further quantum-chemical calculations were carried out on the stability and reactivity of tertiary radical species for polymer forming reactions, which we discuss in the next section.

Reversible Elimination Reactions from Tertiary Methyl Styryl Radical Species. A deeper assessment of the tertiary radical species (7, Figure Sa) formed by the thiyl addition to MeSty revealed four very different reaction pathways. Most notably is the reversible elimination processes back to MeSty

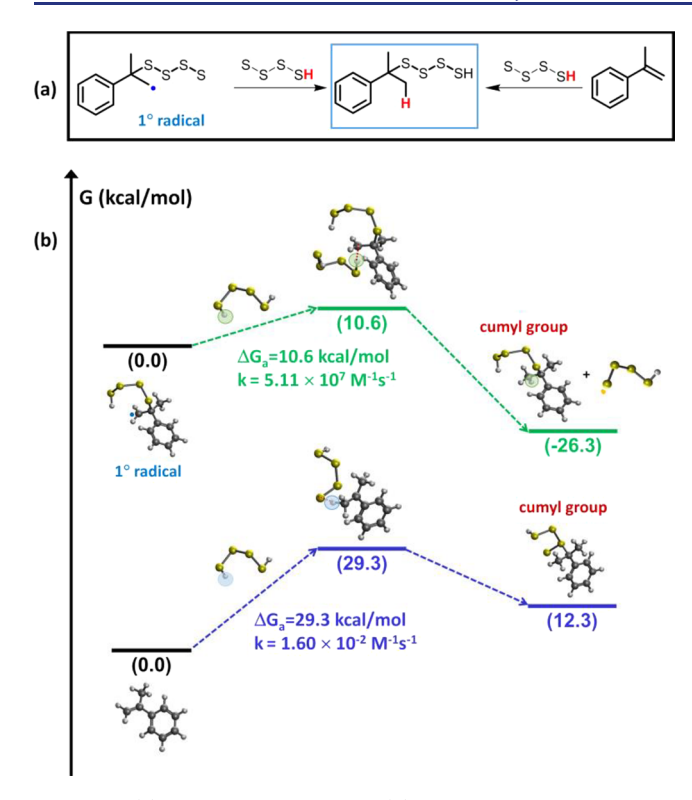


Figure 6. (a) Synthetic scheme and (b) reaction coordinate for the formation of thio-cumyl units via HSSSS radical abstraction or direct addition to a-methyl styrene.

olefin +HSSSS thiyl radicals (Figure 5a), which was calculated to be the most favorable and fastest process ($\Delta G_a^{\ddagger} = 7.6 \text{ kcal/}$ mol; $k = 1.44 \times 10^9$ L/mol s); in addition, the cyclization of the same tertiary radical intermediate (Figure 5b) to form a thiirane had slighter lower exergonicity ($\Delta G = -8.9 \text{ kcal/mol}$ for cyclization vs -9.5 kcal/mol for elimination) and slightly lower rates ($\Delta G_a^{\ddagger} = 12.9 \text{ kcal/mol}$; $k = 2.87 \times 10^6 \text{ L/mol s}$). Nevertheless, the exergonicity and fast rate of these elimination processes revealed that this tertiary radical species is not a viable intermediate for the C-S bond-forming reactions required for inverse vulcanization. This conclusion was further supported by calculations of the tertiary radical ring-opening addition to S₈ (Figure 5c), which proceeded with a higher energetic barrier (19.2 kcal/mol) and led to the endergonic $(\Delta G = +2.6 \text{ kcal/mol})$ and much slower $(k = 1.93 \times 10^3 \text{ L/mol})$ mol s) formation of a bis-sulfurated MeSty product with two tetrasulfide units. Furthermore, the H-atom abstraction reaction of thiyl radical species from either allylic- methyl, or methylene positions of the tertiary radical intermediate was evaluated and calculated to proceed via a barrierless, highly exergonic process ($\Delta G = -2\overline{1.3}$ kcal/mol) to form the allylic sulfides (9) or, in a two-step highly exergonic process ($\Delta G =$ -23.4 kcal/mol), to afford vinyl sulfides (10), respectively, depending on sites of abstraction (Figure 5d).

Formation of Thiocumyl Groups via Homolytic vs Heterolytic Processes. Since the results of the calculations illustrated in Figure 5 indicated the preference of tertiary radical intermediates for an elimination-depolymerization process, additional studies were conducted on the primary

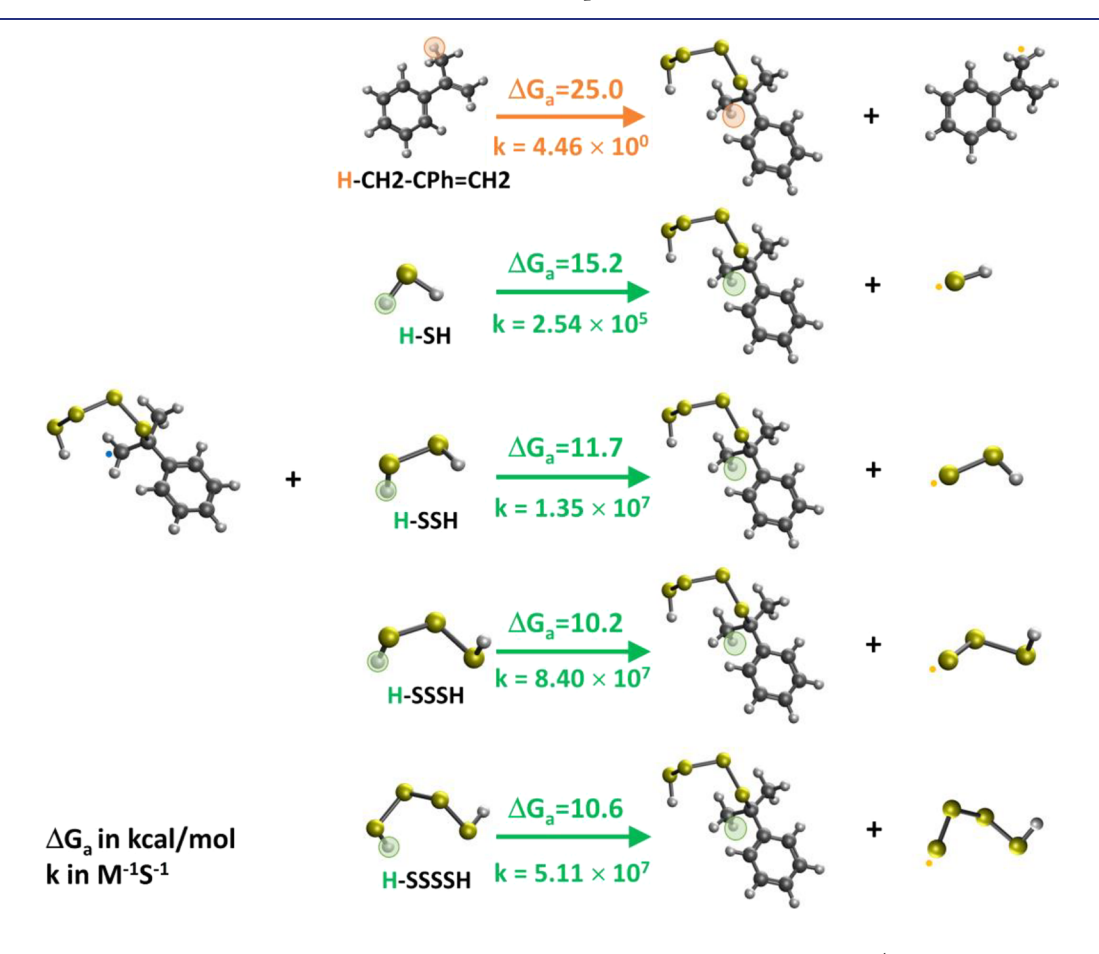


Figure 7. Calculated Gibbs free energies of activation and rate constants for the coupling of primary radicals (derived from thiyl radical addition to MeSty) with HS- species of varying sulfur rank.

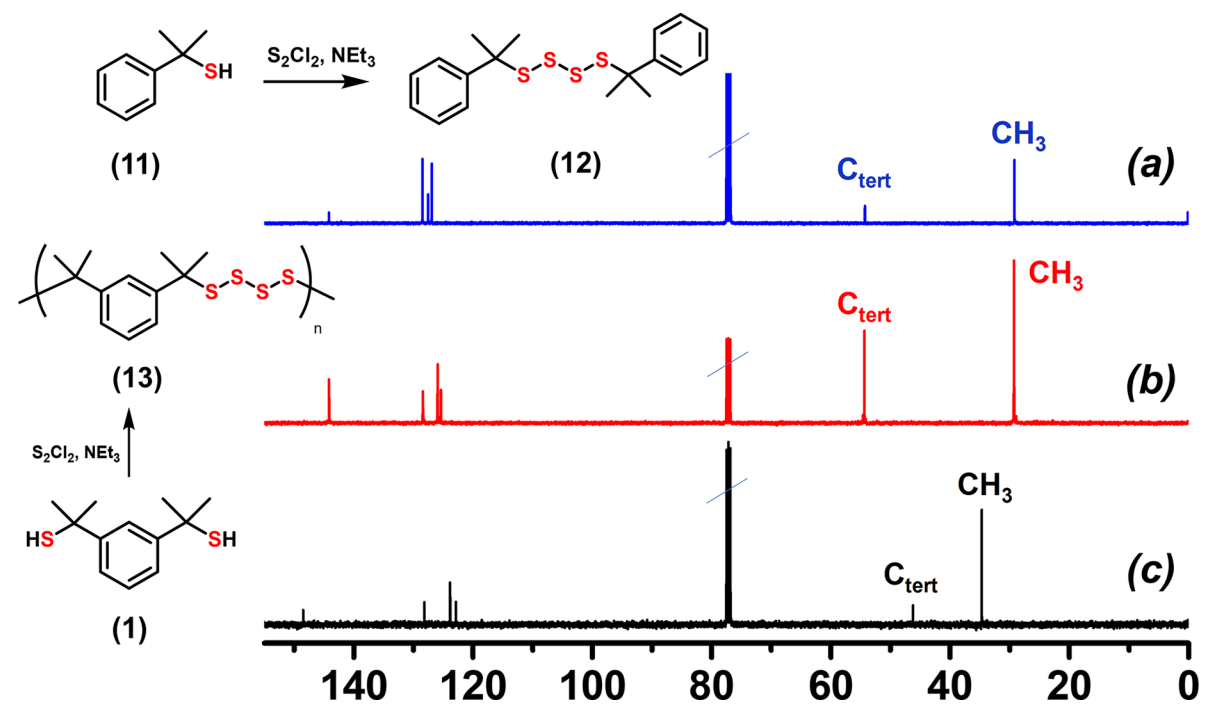


Figure 8. (a) Sulfuration of cumyl thiol 11 with S_2Cl_2 to afford model tetrasulfide 12 and solution-state ^{13}C NMR spectrum of 12, (b) synthesis of linear polytetrasulfide 13 by sulfuration of 1 with S_2Cl_2 and solution-state ^{13}C NMR spectrum of 13, and (c) solution ^{13}C NMR spectrum of biscumyl thiol 1.

radical addition pathway as the most likely process to form thiocumyl microstructures for inverse vulcanization with DIB. The most direct possible mechanistic pathway for forming the observed thiocumyl fragment for HSSSS and MeSty is via termination of the thiocumyl radical by abstraction of a hydrogen atom from a sulfane —SSSSH species (Figure 6a,b), which can be formed by direct abstraction of allylic hydrogens from the methyl position of MeSty (Figure 4b).

This process was calculated to be highly exergonic ($\Delta G =$ -26.3 kcal/mol) and proceeded with a fast reaction rate (k = 5.11×10^7 L/mol s) (Figure 6b). We also evaluated the heterolytic electrophilic addition process of the sulfane HSSSspecies to the olefin of MeSty in a Markovnikov fashion; the resulting pathway was found to be far less favorable (ΔG_a^{\ddagger} = 29.3 kcal/mol, $k = 1.60 \times 10^{-2}$ L/mol s), and thus considered unlikely. Interestingly, the computational results (see Figure 6a) indicated that the barrier for abstraction from HSSSS was 10.6 kcal/mol; this value is significantly lower compared to the scenario wherein the primary radical is terminated by abstracting a hydrogen atom from the allylic fragment (25.0 kcal/mol), leading to a rate difference of almost seven orders of magnitude. Furthermore, and most strikingly, our computational studies highlight that H2S is about two orders of magnitude slower ($\Delta G_{2}^{\ddagger} = 15.2 \text{ kcal/mol}$) in delivering a hydrogen atom to the primary radical in comparison to HSS $(\Delta G_a^{\ddagger} = 11.7 \text{ kcal/mol})$, HSSS $(\Delta G_a^{\ddagger} = 10.2 \text{ kcal/mol})$, and HSSSS ($\Delta G_a^{\ddagger} = 10.6 \text{ kcal/mol}$), see Figure 7.

The overall picture collected from the quantum-chemical calculations shown in Figures 4–7 offers several important mechanistic insights into the inverse vulcanization of sulfur with DIB. These calculations reveal that despite the more favorable thiol-ene type addition of thiyl radical to form tertiary styryl radicals (Figure 4), the resulting elimination of this intermediate back to MeSty (Figure 5) suggests that similar "dead-end" depolymerization processes are observed

for the inverse vulcanization process with tertiary styryl radical species formed from DIB. The reversibility of tertiary methyl styryl radicals is consistent with the low ceiling temperatures $(T_c = 61 \, ^{\circ}\text{C})$ observed in the free radical homo-polymerization of MeSty. 64 Additionally, while allylic H-atom abstraction from the methyl groups of the MeSty monomer is an endergonic, slow process (Figure 4), allylic H-atom abstraction from methyl and methylene groups on tertiary styryl radicals proceeds with high exergonicity and fast rates (Figure 5), which offers two different routes for H-atom abstraction to form H-donor sulfane species. Finally, the homolytic termination of primary radicals (generated from thiyl addition to MeSty) with sulfane H-SSS species was calculated to proceed exergonically to form thiocumyl units (Figure 6), which provides a viable reaction pathway to form thiocumyl units in poly(S-r-DIB). This type of mechanism is consistent with earlier studies reported in the rubber vulcanization literature, where allylic H-abstraction and C-S bond formation is predominantly observed versus C-S bond formation via olefin addition pathways.65

Pending Mechanistic Studies. An unresolved question that is still being investigated is the competitive generation of dithiole thione species via the reaction of elemental sulfur with isopropenyl or α -olefinic molecules versus allylic H-atom abstraction by thiyl radical species. Earlier literature precedence has documented the possibility of both processes to be present, with homolytic allylic hydrogen abstraction reactions dominating at lower temperatures and shorter reaction times. At higher temperatures, it is the conversion of isopropenyl/alkyl propenyl moieties into dithiole thione groups with evolution of H_2S that has been reported to occur. More recently, this has elegantly been experimentally confirmed by Kanbara and co-workers for reactions of S_8 with MeSty, as noted by the formation of the dithiole thione and H_2S . This oxidative process could in principle be a source of H-atoms

 \underline{R} = -SH, Ph-C(CH₃)=CH₂; \underline{X} = CH₃, -S_n-; \underline{Y} = CH₃, H

Figure 9. Proposed complete microstructure of poly(S-r-DIB) synthesized by the inverse vulcanization of S₈ and DIB.

required for thiocumyl fragment formation, but would presume near stoichiometric generation of H2S gas during the inverse vulcanization of S₈ and DIB. While some generation of H₂S has been reported during inverse vulcanization with DIB,⁵³ visible bubbling of the reaction media is not observed under most bulk polymerization conditions, in contrast with inverse vulcanizations of S₈ with 1,3-phenylene diamine, ¹⁸ or reactions that have undergone thermal runaway.³⁵ In our kinetic studies of the inverse vulcanization of S₈ with DIB, we do observe small amounts of dithiole thione as noted by ¹H NMR spectroscopy of bulk polymerization aliquots (see Supporting Information, Figure S42). Hence, it is now evident that dithiole thione formation occurs in the inverse vulcanization with DIB, but the mechanistic pathway to form these species and the role of these reactions to form poly(S-r-DIB) are still unclear and the subject of ongoing research. Our preliminary quantumchemical calculations demonstrate a possible homolytic pathway to dithiole thione formation by exhaustive allylic Hatom abstraction of methyl groups in DIB, followed by subsequent C-S radical coupling and elimination of thiyl radical species from the liquid sulfur phase (see Supporting Information, Figures S43-44).

Synthesis and NMR Spectroscopy of Cumyl Tetrasulfides and Linear Cumyl Polytetrasulfides. Synthetic access to both mono- and bis-cumyl thiols has opened the door for designer preparation of cumyl tetrasulfide model compounds and linear polytetrasulfides which allowed for concrete structure-property comparisons to inverse vulcanization-derived poly(S-r-DIB). Mono-cumyl thiol 11 was prepared by the basic cleavage of the corresponding cumyl thioester and further reacted with sulfur monochloride in the presence of triethylamine to prepare target tetrasulfide 12 (Figure 8a).⁶⁷ Similarly, bis-cumyl thiol 1 was used as an A₂ monomer in a step-growth polymerization with sulfur monochloride (S₂Cl₂ as the B₂ monomer) to prepare linear polysulfide 13 which possesses an exact sulfur rank of 4-sulfur units throughout the polymer chain. SEC in THF confirmed that a polymeric material was formed from this process $(M_n =$ 13,200 g/mol; $M_{\rm w}/M_{\rm n}=2.4$). Synthetic access to both the small molecule and linear polytetrasulfide containing only the thiocumyl units allows for precise comparison of the solution ¹³C NMR spectra of these reference materials to the ¹³C CP-MAS NMR spectra profile of poly(S-r-DIB).

Solution ¹³C NMR spectra of tetrasulfide 12 and linear polysulfide 13 showed both methyl (29 ppm) and C_{tert} (55 ppm) resonances of comparable peak heights, which closely matched the ¹³C NMR spectra of bis-cumyl thiol 1 (Figure 8c) but with these peaks shifted downfield as a consequence of the higher sulfur rank. Linear polysulfide 13 is the perfect linear version of poly(S-r-DIB) composed of only 1,3-phenylene bisthiocumyl units with an exact sulfur rank of four, while poly(S-

r-DIB) derived from inverse vulcanization has a statistical distribution of sulfur ranks and the possibility for other minor repeating unit microstructures. Despite these structural differences, the ¹³C NMR spectra of these various polymers are remarkably similar with respect to the primary number of carbon peaks, chemical shifts, and relative peak heights. The collective assessment of the spectral similarities of these model materials with the insoluble fraction of poly(S-r-DIB) provides further evidence for the newly proposed thiocumyl repeating unit for this copolymer. Further comparison of the bulk properties of linear polytetrasulfide 13 vs poly(S-r-DIB) revealed significant differences in thermal properties ($T_{\rm g~poly6}$ \sim 15 °C vs $T_{\rm g~poly(S-r-DIB)}\sim$ 25 °C from modulated DSC, see Figure S21), which can be attributed to the more controlled linear structure and precise sulfur rank of the linear polytetrasulfide model material. The refractive index of linear polytetrasulfide 13 ($n_{589\text{nm}} = 1.71$, see Figure S22) was found to be slightly lower than those of poly(S-r-DIB) (n > 1.75 for 50-wt % sulfur), ²³ which indicates that poly(S-r-DIB) exhibits comparable sulfur rank to those of these linear polytetrasulfides. A more detailed structure-property comparison of these materials is currently in progress.

Ramifications of Cumyl Dominant Microstructures for Poly(S-r-DIB). The implications of these structural and mechanistic studies are significant for understanding both the fundamental polymerization chemistry aspects of the inverse vulcanization of DIB and the structure-property aspects of this material in comparison to other comonomers. The main conclusion of this comprehensive study is that the complete microstructure of poly(S-r-DIB) made from inverse vulcanization (Figure 9) must now be revised to primarily consist of thiocumyl fragments as the major microstructure unit, followed by minor units composed of thiopropyl fragments, or bisthiopropyl fragments as inferred from the degradation studies in Figure 3. Furthermore, the poly(S-r-DIB) end groups can be inferred to be either -SSH sulfanes, or dangling isopropenyl moieties. As the primary microstructure of this polymer is composed of the thiocumyl units, for technical communicative purposes, it is recommended to present the chemical repeating unit of poly(S-r-DIB) prepared by inverse vulcanization as shown in Figure 1b. The important role of allylic hydrogen abstraction in the inverse vulcanization of DIB has further been supported by a recent report on the inverse vulcanization of tris-isopropylbenzene¹¹ where abstraction of benzylic H-atoms has afforded polymeric materials with NMR spectroscopic profiles similar to those described herein. Finally, it is further recommended that all new sulfur derived polymers (i.e., inverse vulcanized polymers) include both NMR spectroscopic characterization of the polymer (either solution or solid state), along with analytical structural characterization of degraded organic comonomer units, as detailed in this report. This utility of this approach has effectively been demonstrated for

characterization of inverse vulcanized derived polymers from dicyclopentadiene. 68 Furthermore, this comprehensive characterization protocol holds promise for new S_8 derived organopolysulfides prepared via thiirane- S_8 ring opening copolymerizations. 69 It is important to note that different mechanistic pathways will likely be observed with different organic comonomers, which warrant detailed structural analysis as described herein.

CONCLUSIONS

Comprehensive structural and mechanistic studies were conducted on poly(S-r-DIB) copolymers prepared by inverse vulcanization using solution and solid-state ¹³C NMR spectroscopy. A combination of solid-state NMR spectroscopic analysis of the insoluble polymer, along with polymer degradation studies and synthesis of model compounds, highlights that the predominant repeating unit in poly(S-r-DIB) is composed of thiocumyl units formed during inverse vulcanization. This unexpected microstructure is further supported by the results of quantum-chemical calculations that describe the possible reaction pathways to form this thiocumyl repeating unit and further clarify why the previously proposed thiol-ene type addition mechanism is not observed. Our findings indicate that the previously reported "idealized" microstructures for poly(S-r-DIB) are not predominant, which represents a major outcome in the field of sulfur polymer chemistry. Our results have profound implications on the understanding of the structure-property relationships of the polymeric materials prepared from inverse vulcanization and provide new mechanistic insights into this process. Additional studies are in progress with other well-established organic comonomers for inverse vulcanization, with the goal of establishing more predictable comonomer structural landscape that is well matched for inverse vulcanization and our many long-term application goals with new S₈ derived polymeric materials.

ASSOCIATED CONTENT

Supporting Information

The Supporting Information is available free of charge at https://pubs.acs.org/doi/10.1021/jacs.3c03604.

Full experimental and characterization details, ¹H spectra, ¹³C spectra, ¹H NMR and ¹³C NMR spectra, SEC chromatograms, and thermogravimetric analysis and differential scanning calorimetry results (PDF)

AUTHOR INFORMATION

Corresponding Authors

Wallace O'Neil Parker, Jr. — Physical Chemistry Department, Eni, Research & Technical Innovation, ENI S.p.A., 20097 San Donato Milanese, Italy; oorcid.org/0000-0002-2944-8533; Email: wallace.parker@eni.com

Jon T. Njardarson – Department of Chemistry and Biochemistry, University of Arizona, Tucson, Arizona 85721, United States; orcid.org/0000-0003-2268-1479; Email: njardars@arizona.edu

Jeffrey Pyun — Department of Chemistry and Biochemistry and Wyant College of Optical Sciences, University of Arizona, Tucson, Arizona 85721, United States; orcid.org/0000-0002-1288-8989; Email: jpyun@arizona.edu

Authors

Jianhua Bao – Department of Chemistry and Biochemistry, University of Arizona, Tucson, Arizona 85721, United States Kaitlyn P. Martin – Department of Chemistry and Biochemistry, University of Arizona, Tucson, Arizona 85721, United States

Eunkyung Cho – Department of Chemistry and Biochemistry, University of Arizona, Tucson, Arizona 85721, United States; Occid.org/0000-0001-8501-0029

Kyung-Seok Kang — Department of Chemistry and Biochemistry, University of Arizona, Tucson, Arizona 85721, United States

Richard S. Glass – Department of Chemistry and Biochemistry, University of Arizona, Tucson, Arizona 85721, United States

Veaceslav Coropceanu — Department of Chemistry and Biochemistry, University of Arizona, Tucson, Arizona 85721, United States; orcid.org/0000-0003-1693-2315

Jean-Luc Bredas — Department of Chemistry and Biochemistry, University of Arizona, Tucson, Arizona 85721, United States; Occid.org/0000-0001-7278-4471

Complete contact information is available at: https://pubs.acs.org/10.1021/jacs.3c03604

Author Contributions

All authors have given approval to the final version of the manuscript.

Notes

The authors declare no competing financial interest.

ACKNOWLEDGMENTS

We gratefully acknowledge the National Science Foundation and the Air Force Research Laboratory through DMREF-2118578, the National Science Foundation (PFI-RP 1940942 and MRI-1920234), the Air Force Research Laboratories (FA8650-16-D-5404), the RII Research Advancement Grant program from the University of Arizona, the Arizona Technology and Research Initiative Fund (A.R.S.§15-1648), and ENI S.p.A for supporting this work.

■ REFERENCES

- (1) Lim, J.; Pyun, J.; Char, K. Recent Approaches for the Direct Use of Elemental Sulfur in the Synthesis and Processing of Advanced Materials. *Angew. Chem., Int. Ed.* **2015**, *54*, 3249–3258.
- (2) Griebel, J. J.; Glass, R. S.; Char, K.; Pyun, J. Polymerizations with elemental sulfur: A novel route to high sulfur content polymers for sustainability, energy and defense. *Prog. Polym. Sci.* **2016**, *58*, 90–125.
- (3) Lee, T.; Dirlam, P. T.; Njardarson, J. T.; Glass, R. S.; Pyun, J. Polymerizations with Elemental Sulfur: From Petroleum Refining to Polymeric Materials. *J. Am. Chem. Soc.* **2022**, *144*, 5–22.
- (4) Penczek, S.; SLazak, R.; Duda, A. Anionic copolymerisation of elemental sulphur. *Nature* **1978**, *273*, 738–739.
- (5) Duda, A.; Penczek, S. Anionic copolymerization of elemental sulfur with propylene sulfide. *Macromolecules* **1982**, *15*, 36–40.
- (6) Meyer, B. Elemental sulfur. Chem. Rev. 1976, 76, 367–388.
- (7) Zhang, Y.; Glass, R. S.; Char, K.; Pyun, J. Recent advances in the polymerization of elemental sulphur, inverse vulcanization and methods to obtain functional Chalcogenide Hybrid Inorganic/Organic Polymers (CHIPs). *Polym. Chem.* **2019**, *10*, 4078–4105.
- (8) Chung, W. J.; Griebel, J. J.; Kim, E. T.; Yoon, H.; Simmonds, A. G.; Ji, H. J.; Dirlam, P. T.; Glass, R. S.; Wie, J. J.; Nguyen, N. A.; Guralnick, B. W.; Park, J.; Somogyi, Á.; Theato, P.; Mackay, M. E.; Sung, Y.-E.; Char, K.; Pyun, J. The use of elemental sulfur as an

- alternative feedstock for polymeric materials. *Nat. Chem.* **2013**, *5*, 518–524.
- (9) Worthington, M. J. H.; Kucera, R. L.; Chalker, J. M. Green chemistry and polymers made from sulfur. *Green Chem.* **2017**, *19*, 2748–2761.
- (10) Chalker, J. M.; Worthington, M. J. H.; Lundquist, N. A.; Esdaile, L. J. Synthesis and Applications of Polymers Made by Inverse Vulcanization. *Top. Curr. Chem.* **2019**, *377*, 16.
- (11) Lai, Y.-S.; Liu, Y.-L. Reaction between 1,3,5-Triisopropylbenzene and Elemental Sulfur Extending the Scope of Reagents in Inverse Vulcanization. *Macromol. Rapid Commun.* **2023**, *44*, No. 2300014.
- (12) Zhang, Y.; Konopka, K. M.; Glass, R. S.; Char, K.; Pyun, J. Chalcogenide hybrid inorganic/organic polymers (CHIPs) via inverse vulcanization and dynamic covalent polymerizations. *Polym. Chem.* **2017**, *8*, 5167–5173.
- (13) Westerman, C. R.; Jenkins, C. L. Dynamic Sulfur Bonds Initiate Polymerization of Vinyl and Allyl Ethers at Mild Temperatures. *Macromolecules* **2018**, *51*, 7233–7238.
- (14) Zhang, Y.; Kleine, T. S.; Carothers, K. J.; Phan, D. D.; Glass, R. S.; Mackay, M. E.; Char, K.; Pyun, J. Functionalized chalcogenide hybrid inorganic/organic polymers (CHIPs) via inverse vulcanization of elemental sulfur and vinylanilines. *Polym. Chem.* **2018**, *9*, 2290–2294.
- (15) Kang, K.-S.; Phan, A.; Olikagu, C.; Lee, T.; Loy, D. A.; Kwon, M.; Paik, H.-J.; Hong, S. J.; Bang, J.; Parker, W. O., Jr.; Sciarra, M.; de Angelis, A. R.; Pyun, J. Segmented Polyurethanes and Thermoplastic Elastomers from Elemental Sulfur with Enhanced Thermomechanical Properties and Flame Retardancy. *Angew. Chem., Int. Ed.* **2021**, *60*, 22900–22907.
- (16) Wang, D.; Tang, Z.; Huang, R.; Duan, Y.; Wu, S.; Guo, B.; Zhang, L. Interface Coupling in Rubber/Carbon Black Composites toward Superior Energy-Saving Capability Enabled by Amino-Functionalized Polysulfide. *Chem. Mater.* **2023**, *35*, 764–772.
- (17) Zhang, Y.; Pavlopoulos, N. G.; Kleine, T. S.; Karayilan, M.; Glass, R. S.; Char, K.; Pyun, J. Nucleophilic Activation of Elemental Sulfur for Inverse Vulcanization and Dynamic Covalent Polymerizations. J. Polym. Sci. Part A: Polym. Chem. 2019, 57, 7–12.
- (18) Karayilan, M.; Kleine, T. S.; Carothers, K. J.; Griebel, J. J.; Frederick, K. M.; Loy, D. A.; Glass, R. S.; Mackay, M. E.; Char, K.; Pyun, J. Chalcogenide hybrid inorganic/organic polymer resins: Amine functional prepolymers from elemental sulfur. *J. Polym. Sci.* **2020**, *58*, 35–41.
- (19) Wu, X.; Smith, J. A.; Petcher, S.; Zhang, B.; Parker, D. J.; Griffin, J. M.; Hasell, T. Catalytic inverse vulcanization. *Nat. Commun.* **2019**, *10*, 647.
- (20) Dodd, L. J.; Omar, Ö.; Wu, X.; Hasell, T. Investigating the Role and Scope of Catalysts in Inverse Vulcanization. *ACS Catal.* **2021**, *11*, 4441–4455.
- (21) Ambulo, C. P.; Carothers, K. J.; Hollis, A. T.; Limburg, H. N.; Sun, L.; Thrasher, C. J.; McConney, M. E.; Godman, N. P. Photo-Crosslinkable Inorganic/Organic Sulfur Polymers. *Macromol. Rapid Commun.* **2023**, *44*, No. 2200798.
- (22) Jia, J.; Liu, J.; Wang, Z.-Q.; Liu, T.; Yan, P.; Gong, X.-Q.; Zhao, C.; Chen, L.; Miao, C.; Zhao, W.; Cai, S.; Wang, X.-C.; Cooper, A. I.; Wu, X.; Hasell, T.; Quan, Z.-J. Photoinduced inverse vulcanization. *Nat. Chem.* **2022**, *14*, 1249–1257.
- (23) Griebel, J. J.; Namnabat, S.; Kim, E. T.; Himmelhuber, R.; Moronta, D. H.; Chung, W. J.; Simmonds, A. G.; Kim, K.-J.; van der Laan, J.; Nguyen, N. A.; Dereniak, E. L.; Mackay, M. E.; Char, K.; Glass, R. S.; Norwood, R. A.; Pyun, J. New Infrared Transmitting Material via Inverse Vulcanization of Elemental Sulfur to Prepare High Refractive Index Polymers. *Adv. Mater.* 2014, 26, 3014–3018.
- (24) Griebel, J. J.; Nguyen, N. A.; Namnabat, S.; Anderson, L. E.; Glass, R. S.; Norwood, R. A.; Mackay, M. E.; Char, K.; Pyun, J. Dynamic Covalent Polymers via Inverse Vulcanization of Elemental Sulfur for Healable Infrared Optical Materials. *ACS Macro Lett.* **2015**, *4*, 862–866.
- (25) Kleine, T. S.; Nguyen, N. A.; Anderson, L. E.; Namnabat, S.; LaVilla, E. A.; Showghi, S. A.; Dirlam, P. T.; Arrington, C. B.;

- Manchester, M. S.; Schwiegerling, J.; Glass, R. S.; Char, K.; Norwood, R. A.; Mackay, M. E.; Pyun, J. High Refractive Index Copolymers with Improved Thermomechanical Properties via the Inverse Vulcanization of Sulfur and 1,3,5-Triisopropenylbenzene. *ACS Macro Lett.* **2016**, *5*, 1152–1156
- (26) Anderson, L. E.; Kleine, T. S.; Zhang, Y.; Phan, D. D.; Namnabat, S.; LaVilla, E. A.; Konopka, K. M.; Ruiz Diaz, L.; Manchester, M. S.; Schwiegerling, J.; Glass, R. S.; Mackay, M. E.; Char, K.; Norwood, R. A.; Pyun, J. Chalcogenide Hybrid Inorganic/Organic Polymers: Ultrahigh Refractive Index Polymers for Infrared Imaging. ACS Macro Lett. 2017, 6, 500–504.
- (27) Boyd, D. A.; Baker, C. C.; Myers, J. D.; Nguyen, V. Q.; Drake, G. A.; McClain, C. C.; Kung, F. H.; Bowman, S. R.; Kim, W.; Sanghera, J. S. ORMOCHALCs: organically modified chalcogenide polymers for infrared optics. *Chem. Commun.* **2017**, *53*, 259–262.
- (28) Kleine, T. S.; Diaz, L. R.; Konopka, K. M.; Anderson, L. E.; Pavlopolous, N. G.; Lyons, N. P.; Kim, E. T.; Kim, Y.; Glass, R. S.; Char, K.; Norwood, R. A.; Pyun, J. One Dimensional Photonic Crystals Using Ultrahigh Refractive Index Chalcogenide Hybrid Inorganic/Organic Polymers. ACS Macro Lett. 2018, 7, 875–880.
- (29) Boyd, D. A.; Nguyen, V. Q.; McClain, C. C.; Kung, F. H.; Baker, C. C.; Myers, J. D.; Hunt, M. P.; Kim, W.; Sanghera, J. S. Optical Properties of a Sulfur-Rich Organically Modified Chalcogenide Polymer Synthesized via Inverse Vulcanization and Containing an Organometallic Comonomer. ACS Macro Lett. 2019, 8, 113–116. (30) Kleine, T. S.; Lee, T.; Carothers, K. J.; Hamilton, M. O.; Anderson, L. E.; Ruiz Diaz, L.; Lyons, N. P.; Coasey, K. R.; Parker, W. O., Jr.; Borghi, L.; Mackay, M. E.; Char, K.; Glass, R. S.; Lichtenberger, D. L.; Norwood, R. A.; Pyun, J. Infrared Fingerprint Engineering: A Molecular-Design Approach to Long-Wave Infrared Transparency with Polymeric Materials. Angew. Chem., Int. Ed. 2019, 58, 17656–17660.
- (31) Lee, J. M.; Noh, G. Y.; Kim, B. G.; Yoo, Y.; Choi, W. J.; Kim, D.-G.; Yoon, H. G.; Kim, Y. S. Synthesis of Poly(phenylene polysulfide) Networks from Elemental Sulfur and p-Diiodobenzene for Stretchable, Healable, and Reprocessable Infrared Optical Applications. ACS Macro Lett. 2019, 8, 912–916.
- (32) Kleine, T. S.; Glass, R. S.; Lichtenberger, D. L.; Mackay, M. E.; Char, K.; Norwood, R. A.; Pyun, J. 100th Anniversary of Macromolecular Science Viewpoint: High Refractive Index Polymers from Elemental Sulfur for Infrared Thermal Imaging and Optics. ACS Macro Lett. 2020, 9, 245–259.
- (33) Simmonds, A. G.; Griebel, J. J.; Park, J.; Kim, K. R.; Chung, W. J.; Oleshko, V. P.; Kim, J.; Kim, E. T.; Glass, R. S.; Soles, C. L.; Sung, Y.-E.; Char, K.; Pyun, J. Inverse Vulcanization of Elemental Sulfur to Prepare Polymeric Electrode Materials for Li–S Batteries. *ACS Macro Lett.* **2014**, *3*, 229–232.
- (34) Dirlam, P. T.; Simmonds, A. G.; Kleine, T. S.; Nguyen, N. A.; Anderson, L. E.; Klever, A. O.; Florian, A.; Costanzo, P. J.; Theato, P.; Mackay, M. E.; Glass, R. S.; Char, K.; Pyun, J. Inverse vulcanization of elemental sulfur with 1,4-diphenylbutadiyne for cathode materials in Li–S batteries. *RSC Adv.* **2015**, *5*, 24718–24722.
- (35) Griebel, J. J.; Li, G.; Glass, R. S.; Char, K.; Pyun, J. Kilogram scale inverse vulcanization of elemental sulfur to prepare high capacity polymer electrodes for Li-S batteries. *J. Polym. Sci. Part A Polym. Chem.* **2015**, *53*, 173–177.
- (36) Arslan, M.; Kiskan, B.; Cengiz, E. C.; Demir-Cakan, R.; Yagci, Y. Inverse vulcanization of bismaleimide and divinylbenzene by elemental sulfur for lithium sulfur batteries. *Eur. Polym. J.* **2016**, *80*, 70–77.
- (37) Dirlam, P. T.; Park, J.; Simmonds, A. G.; Domanik, K.; Arrington, C. B.; Schaefer, J. L.; Oleshko, V. P.; Kleine, T. S.; Char, K.; Glass, R. S.; Soles, C. L.; Kim, C.; Pinna, N.; Sung, Y.-E.; Pyun, J. Elemental Sulfur and Molybdenum Disulfide Composites for Li–S Batteries with Long Cycle Life and High-Rate Capability. *ACS Appl. Mater. Interfaces* **2016**, *8*, 13437–13448.
- (38) Gomez, I.; Leonet, O.; Blazquez, J. A.; Mecerreyes, D. Inverse Vulcanization of Sulfur using Natural Dienes as Sustainable Materials for Lithium—Sulfur Batteries. *ChemSusChem* **2016**, *9*, 3419—3425.

- (39) Gomez, I.; Mecerreyes, D.; Blazquez, J. A.; Leonet, O.; Ben Youcef, H.; Li, C.; Gómez-Cámer, J. L.; Bondarchuk, O.; Rodriguez-Martinez, L. Inverse vulcanization of sulfur with divinylbenzene: Stable and easy processable cathode material for lithium-sulfur batteries. J. Power Sources 2016, 329, 72-78.
- (40) Dirlam, P. T.; Glass, R. S.; Char, K.; Pyun, J. The use of polymers in Li-S batteries: A review. J. Polym. Sci. Part A Polym. Chem. 2017, 55, 1635-1668.
- (41) Griebel, J. J.; Nguyen, N. A.; Astashkin, A. V.; Glass, R. S.; Mackay, M. E.; Char, K.; Pyun, J. Preparation of Dynamic Covalent Polymers via Inverse Vulcanization of Elemental Sulfur. ACS Macro Lett. 2014, 3, 1258-1261.
- (42) Tonkin, S. J.; Gibson, C. T.; Campbell, J. A.; Lewis, D. A.; Karton, A.; Hasell, T.; Chalker, J. M. Chemically induced repair, adhesion, and recycling of polymers made by inverse vulcanization. Chem. Sci. 2020, 11, 5537-5546.
- (43) Yan, P.; Zhao, W.; Zhang, B.; Jiang, L.; Petcher, S.; Smith, J. A.; Parker, D. J.; Cooper, A. I.; Lei, J.; Hasell, T. Inverse Vulcanized Polymers with Shape Memory, Enhanced Mechanical Properties, and Vitrimer Behavior. Angew. Chem., Int. Ed. 2020, 59, 13371-13378.
- (44) Crockett, M. P.; Evans, A. M.; Worthington, M. J. H.; Albuquerque, I. S.; Slattery, A. D.; Gibson, C. T.; Campbell, J. A.; Lewis, D. A.; Bernardes, G. J. L.; Chalker, J. M. Sulfur-Limonene Polysulfide: A Material Synthesized Entirely from Industrial By-Products and Its Use in Removing Toxic Metals from Water and Soil. Angew. Chem., Int. Ed. 2016, 55, 1714-1718.
- (45) Lundquist, N. A.; Worthington, M. J. H.; Adamson, N.; Gibson, C. T.; Johnston, M. R.; Ellis, A. V.; Chalker, J. M. Polysulfides made from re-purposed waste are sustainable materials for removing iron from water. RSC Adv. 2018, 8, 1232-1236.
- (46) Worthington, M. J. H.; Shearer, C. J.; Esdaile, L. J.; Campbell, J. A.; Gibson, C. T.; Legg, S. K.; Yin, Y.; Lundquist, N. A.; Gascooke, J. R.; Albuquerque, I. S.; Shapter, J. G.; Andersson, G. G.; Lewis, D. A.; Bernardes, G. J. L.; Chalker, J. M. Sustainable Polysulfides for Oil Spill Remediation: Repurposing Industrial Waste for Environmental Benefit. Adv. Sustain. Syst. 2018, 2, No. 1800024.
- (47) Tikoalu, A. D.; Lundquist, N. A.; Chalker, J. M. Mercury Sorbents Made By Inverse Vulcanization of Sustainable Triglycerides: The Plant Oil Structure Influences the Rate of Mercury Removal from Water. Adv. Sustain. Syst. 2020, 4, No. 1900111.
- (48) Mann, M.; Kruger, J. E.; Andari, F.; McErlean, J.; Gascooke, J. R.; Smith, J. A.; Worthington, M. J. H.; McKinley, C. C. C.; Campbell, J. A.; Lewis, D. A.; Hasell, T.; Perkins, M. V.; Chalker, J. M. Sulfur polymer composites as controlled-release fertilisers. Org. Biomol. Chem. 2019, 17, 1929-1936.
- (49) Herrera, C.; Ysinga, K. J.; Jenkins, C. L. Polysulfides Synthesized from Renewable Garlic Components and Repurposed Sulfur Form Environmentally Friendly Adhesives. ACS Appl. Mater. Interfaces 2019, 11, 35312-35318.
- (50) Wang, D.; Tang, Z.; Huang, R.; Li, H.; Zhang, C.; Guo, B. Inverse Vulcanization of Vinyltriethoxysilane: A Novel Interfacial Coupling Agent for Silica-Filled Rubber Composites. Macromolecules 2022, 55, 8485-8494.
- (51) Kang, K.-S.; Iyer, K. A.; Pyun, J. On the Fundamental Polymer Chemistry of Inverse Vulcanization for Statistical and Segmented Copolymers from Elemental Sulfur. Chem. - Eur. J. 2022, 28, No. e202200115.
- (52) Hoefling, A.; Nguyen, D. T.; Partovi-Azar, P.; Sebastiani, D.; Theato, P.; Song, S.-W.; Lee, Y. J. Mechanism for the Stable Performance of Sulfur-Copolymer Cathode in Lithium-Sulfur Battery Studied by Solid-State NMR Spectroscopy. Chem. Mater. 2018, 30, 2915-2923.
- (53) Shankarayya Wadi, V. K.; Jena, K. K.; Khawaja, S. Z.; Yannakopoulou, K.; Fardis, M.; Mitrikas, G.; Karagianni, M.; Papavassiliou, G.; Alhassan, S. M. NMR and EPR Structural Analysis and Stability Study of Inverse Vulcanized Sulfur Copolymers. ACS Omega 2018, 3, 3330-3339.

- (54) Poulain, S.; Julien, S.; Duñach, E. Conversion of norbornene derivatives into vicinal-dithioethers via S8 activation. Tetrahedron Lett. 2005, 46, 7077-7079.
- (55) Chapovetsky, A.; Haiges, R.; Marinescu, S. C. Synthesis and characterization of a tetranickel complex supported by a dithiolate framework with pendant ether moieties. Polyhedron 2017, 123, 9-13.
- (56) Gauthier, J. Y.; Bourdon, F.; Young, R. N. A mild and efficient synthesis of thiolesters from alcohols. Tetrahedron Lett. 1986, 27, 15-
- (57) Burgess, E. M.; Penton, H. R., Jr.; Taylor, E. A. Thermal reactions of alkyl N-carbomethoxysulfamate esters. J. Org. Chem. 1973, 38, 26-31.
- (58) Chauvin, J.-P. R.; Griesser, M.; Pratt, D. A. Hydropersulfides: H-Atom Transfer Agents Par Excellence. J. Am. Chem. Soc. 2017, 139,
- (59) Zhang, Y.; Griebel, J. J.; Dirlam, P. T.; Nguyen, N. A.; Glass, R. S.; Mackay, M. E.; Char, K.; Pyun, J. Inverse vulcanization of elemental sulfur and styrene for polymeric cathodes in Li-S batteries. J. Polym. Sci., Part A: Polym. Chem. 2017, 55, 107-116.
- (60) Frisch, M. J.; Trucks, G. W.; Schlegel, H. B.; Scuseria, G. E.; Robb, M. A.; Cheeseman, J. R.; Scalmani, G.; Barone, V.; Petersson, G. A.; Nakatsuji, H.; Li, X.; Caricato, M.; Marenich, A. V.; Bloino, J.; Janesko, B. G.; Gomperts, R.; Mennucci, B.; Hratchian, H. P.; Ortiz, J. V.; Izmaylov, A. F.; Sonnenberg, J. L.; Williams-Young, D.; Ding, F.; Lipparini, F.; Egidi, F.; Goings, J.; Peng, B.; Petrone, A.; Henderson, T.; Ranasinghe, D.; Zakrzewski, V. G.; Gao, J.; Rega, N.; Zheng, G.; Liang, W.; Hada, M.; Ehara, M.; Toyota, K.; Fukuda, R.; Hasegawa, J.; Ishida, M.; Nakajima, T.; Honda, Y.; Kitao, O.; Nakai, H.; Vreven, T.; Throssell, K.; Montgomery, Jr., J. A.; Peralta, J. E.; Ogliaro, F.; Bearpark, M. J.; Heyd, J. J.; Brothers, E. N.; Kudin, K. N.; Staroverov, V. N.; Keith, T. A.; Kobayashi, R.; Normand, J.; Raghavachari, K.; Rendell, A. P.; Burant, J. C.; Iyengar, S. S.; Tomasi, J.; Cossi, M.; Millam, J. M.; Klene, M.; Adamo, C.; Cammi, R.; Ochterski, J. W.; Martin, R. L.; Morokuma, K.; Farkas, O.; Foresman, J. B.; Fox, D. J. Gaussian 16 Rev. C.01; Wallingford, CT, 2016.
- (61) Muller, E. F.; Hyne, J. B. Thermal decomposition of tri- and tetrasulfanes. J. Am. Chem. Soc. 1969, 91, 1907-1912.
- (62) Wigner, E. Calculation of the Rate of Elementary Association Reactions. J. Chem. Phys. 1937, 5, 720-725.
- (63) Safaei, Z.; Shiroudi, A.; Zahedi, E.; Sillanpä, M. Atmospheric oxidation reactions of imidazole initiated by hydroxyl radicals: kinetics and mechanism of reactions and atmospheric implications. Phys. Chem. Chem. Phys. 2019, 21, 8445-8456.
- (64) Odian, G. Radical Chain Polymerization. In Principles of Polymerization; Odian, G., Ed.; Wiley-Interscience: Hoboken, NJ, 2004; 198-349.
- (65) Porter, M.: Vulcanization of Rubber. In Organic Chemistry of Sulfur; Oae, S., Ed.; Springer US: Boston, MA, 1977, 71-118.
- (66) Onose, Y.; Ito, Y.; Kuwabara, J.; Kanbara, T. Tracking side reactions of the inverse vulcanization process and developing monomer selection guidelines. Polym. Chem. 2022, 13, 5486-5493.
- (67) Chen, S.; Cao, S.; Liu, S.; Wang, S.; Ren, X.; Huang, H.; Wang, X. Metal Free Sandmeyer-Type Reductive Disulfuration of Anilines. ChemRxiv 2021, DOI: 10.26434/chemrxiv.14681061.v1. (accessed 2021-05-28).
- (68) Mann, M.; Zhang, B.; Tonkin, S. J.; Gibson, C. T.; Jia, Z.; Hasell, T.; Chalker, J. M. Processes for coating surfaces with a copolymer made from sulfur and dicyclopentadiene. Polym. Chem. **2022**, 13, 1320-1327.
- (69) Chao, J.-Y.; Yue, T.-J.; Ren, B.-H.; Gu, G.-G.; Lu, X.-B.; Ren, W.-M. Controlled Disassembly of Elemental Sulfur: An Approach to the Precise Synthesis of Polydisulfides. Angew. Chem., Int. Ed. 2022, 61, No. e202115950.